04,06

Influence of the mechanical activation on the structure, dielectric and piezoelectric characteristics of the binary solid solution $(1-x)BiFeO_3 - xBaTiO_3$ $(x = 0.29)$, with bismuth addition

© N.A. Boldyrev[1], L.A. Shilkina[1], A.V. Nagaenko[2], K.M. Zhidel[1], L.A. Reznichenko[1]

[1] Scientific Research Institute of Physics, Southern Federal University, Rostov-on-Don, Russia
[2] NKTB „Piezopribor" SFU, Rostov-on-Don, Russia

E-mail: nboldyrev@sfedu.ru

Received November 20, 2025
Revised December 1, 2025
Accepted December 1, 2025

Ceramic samples of the binary system $(1-x)BiFeO_3-xBaTiO_3 + 2$ wt.% Bi_2O_3 $(x = 0.29)$ were obtained by the conventional solid-phase reaction method with and without mechanical activation. X-ray diffraction studies revealed that the samples have a pseudocubic crystal structure at room temperature. A diffuse phase transition occurred in the temperature range of (650−800) K. Relaxor-like behavior and the smearing of the phase transition in the studied ceramics can be associated with the presence of non-interacting regions with increased content Bi or Ba, different modulation and crystal lattice symmetry. The grain morphology and dielectric characteristics of the selected solid solutions were investigated. The highest piezoelectric coefficient, ~ 120 pC/N, was obtained in the mechanically activated ceramics $0.71BiFeO_3-0.29BaTiO_3 + 2$ wt.% Bi_2O_3.

Keywords: Perovskite multiferroics, dielectric characteristics, piezoelectric characteristics, solid solutions.

DOI: 10.61011/PSS.2025.12.63081.8805-25

1. Introduction

Multiferroics are materials that combine at least two of the so-called „ferro-orders", such as ferroelectric, ferromagnetic, ferroelastic, and ferrotoroidal [1]. Multiferroics have been studied for many years due to their very wide range of possible applications, including the production of high-precision sensors for alternating and permanent magnetic fields (used in navigation systems and electric motors [2]), memory elements (MRAM, Magnetoresistive Random Access Memory) [3], as well as spintronics devices [4], etc. Bismuth ferrite ($BiFeO_3$, or BF) is a representative of this class of materials. It has Curie and Neel temperatures of 1123 and 643 K, respectively, and is considered for use in various magnetoelectric structures. However, its use is limited due to a number of factors. Such factors include the difficulty of obtaining BF in a single-phase state, the presence of Fe^{2+}/Fe^{3+} ions and oxygen vacancies causing leakage currents, as well as a high electric coercive field necessary for the repolarization of domains. Nevertheless, the modification of BF with rare earth elements or the creation of solid solutions (SS) based on BF can stabilize the structure and improve the characteristics of the resulting materials [5–7]. Among $BiFeO_3$-based SS, the lead-free $BiFeO_3$-$BaTiO_3$ (BF-BT) system has been proposed as a replacement for ceramics based on lead zirconate titanate (PZT). PZT ceramics are widely used in piezoelectric devices due to their excellent dielectric and piezoelectric characteristics near the region of coexistence of rhombohedral (Rh) and tetragonal (T) phases (the so-called morphotropic region, MR) [8,9]. The Curie temperature (T_C) of commercial PZT ceramics ranges from 450 to 770 K, depending on the composition. However, there is a growing need for devices with a wider operating range due to the development of modern industry. BF-BT SS with a low BT content exhibit values of T_C exceeding 650 K, indicating their potential for high-temperature applications of [10]. In addition, the characteristics of SS can be improved by modifying [11] and using mechanical activation (MA) [12] in the ceramic production process.

One of the factors preventing the production of high performance pure BF-based SS is the volatility of bismuth oxide Bi_2O_3, which at sintering temperatures leads to a violation of the stoichiometric ratio of reagents and the formation of an impurity phase of mullite $Bi_2Fe_4O_9$. These flaws can be eliminated by using mechanical activation and adding excess Bi_2O_3 (both individually and together). In this regard, the establishment of patterns of formation of structural, dielectric and piezoelectric characteristics in mechanically activated SS of the composition $BiFeO_3$-$BaTiO_3$ with a superstoichiometric additive Bi_2O_3 is relevant, which became the goal of this work.

2. Objects and methods of study

Ceramic samples of the binary system $(1-x)BiFeO_3-xBaTiO_3 + 2$ wt.% Bi_2O_3 $(x = 0.29)$,

manufactured with and without the use of MA (BFBTm) were the objects of the study. The samples were obtained by double solid-phase synthesis at $T_1 = 1123$ K ($\tau_1 = 10$ h.), $T_2 = 1143$ K ($\tau_2 = 10$ h.) followed by sintering at temperature, $T_{\text{sint.}}$, equal to 1323 K for $\tau_{\text{sint.}} = 2$ h. The initial reagents were Bi_2O_3, Fe_2O_3, TiO_2, $BaCO_3$ with a base substance content of at least 99.95 %. The samples were sintered in the form of discs with diameters $\varnothing = 10$ mm and $h = 1$ mm.

Mechanical activation was carried out at the stage of manufacturing press powders prepared for sintering. A high-energy AGO-2 ball mill manufactured by „NOVITS“ (Novosibirsk, Russia) was used for this purpose. The prepared powder was loaded into drums with an inner diameter of 63 mm together with balls of ZrO_2 with a diameter of 8 mm and a total weight of 200 g. The drum with the mixture was placed in an AGO-2 planetary mill. Grinding was carried out in an alcohol medium for 15 min, the drum rotation speed was 1800 revs/min.

After mechanical treatment, electrodes were applied to the flat surfaces of the discs by stepwise burning of a silver-containing paste: at 473 K for 20 min at 773 K for 30 min and at 1073 K for 20 min.

The X-ray examination was performed by powder diffraction on a DRON-3 diffractometer (Bragg-Brentano focusing) using Co Kα radiation.

The microstructure of sintered ceramics was evaluated using a scanning electron microscope JSM-6390L.

The temperature dependences of the complex permittivity $\varepsilon^* = \varepsilon' - i\varepsilon''$ (ε' and ε'' — the real and imaginary parts of the complex permittivity ε^*, respectively) were measured at $T = (300-900)$ K in the frequency range (10 Hz–100 kHz) using the Agilent 4980A LCR meter. The samples were polarized at $T = 400$ K in a polyethylene siloxane liquid with an external field of 3–6 kV. The piezoelectric characteristics were measured at a frequency of $f = 110$ Hz using a quasi-static piezoelectric module meter d_{33} YE2730A (APC International Ltd, USA).

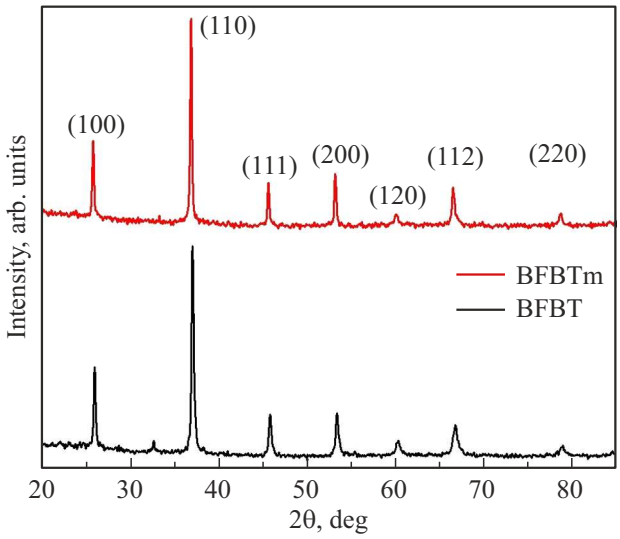

Figure 1. X-ray pattern of BFBT and BFBTm SS.

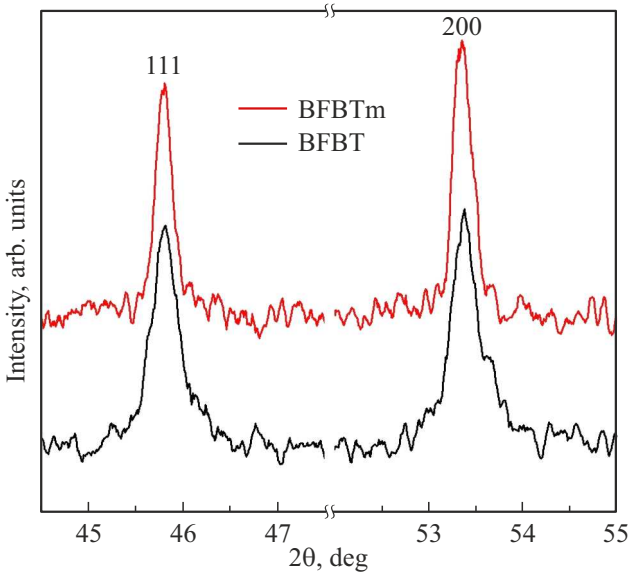

Figure 2. Diffraction peaks 111 and 200 of BFBT and BFBTm SS.

3. Results and discussion

Figure 1 shows X-ray diffraction patterns of the studied ceramics in the angle range of $20 \le 2\theta \le 85$ (°). X-ray patterns of non-mechanically activated BFBT exhibit weak peaks of the impurity phase $Ba_5Fe_2O_8$. After MA, the peaks of the impurity phase disappeared. No distortion of diffraction reflections corresponding to any one symmetry was found, therefore all ceramics have pseudocubic symmetry.

Figure 2 shows the diffraction peaks $\langle 111 \rangle$ and $\langle 200 \rangle$ for the studied samples. Diffuse scattering is observed at the base of the diffraction peaks $\langle 111 \rangle$ and $\langle 200 \rangle$, indicating the presence of atomic segregation. This means that there are regions in the crystal structure whose chemical composition differs from that of the main matrix. The diffuse maxima are blurred, indicating some order in the arrangement of these segregated regions. In mechanically activated ceramics, the signs of atomic segregation disappeared, but splitting appeared in the upper part of the diffraction peaks. This suggests that after MA, there was a more uniform distribution of BT in the BF matrix, which led to the formation of two SS with similar cell parameters.

Figure 3 shows micrographs of the chips of the ceramics under study. The microstructure of the BFBT sample (Figure 3, *a*) mainly consists of two types of grains: small grains with a diameter of less than 1.5 μm, which form compact segregations, and larger grains with a size of more than 3 μm having the shape of irregular polyhedra (Figure 3, *a*). This separation is typical for the microstructure of compositions

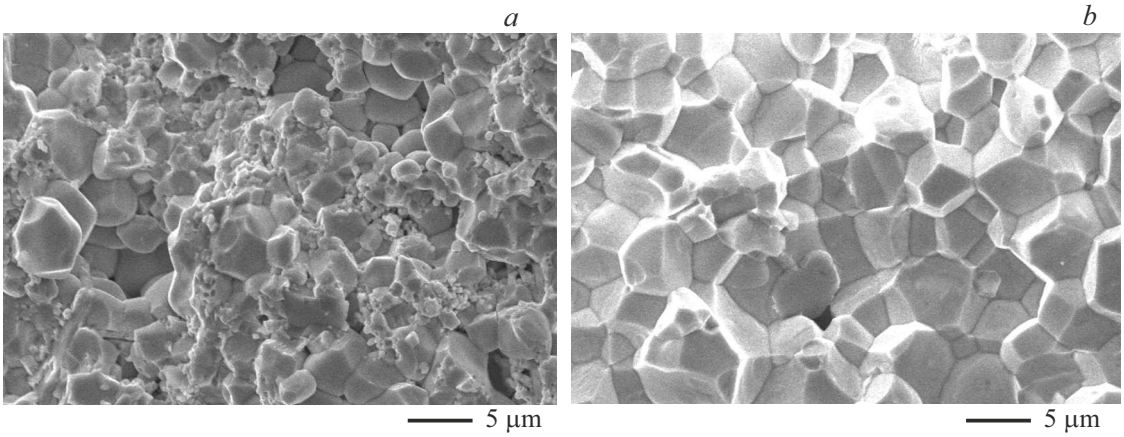

Figure 3. Micrographs of chips of BFBT (*a*) and BFBTm ceramics (*b*).

in which incomplete dissolution of the components has occurred, which is confirmed by data from studies of the crystal structure.

The microstructure of the BFBTm sample is more homogeneous (Figure 3, *b*), the chipping in ceramics passes mainly along the grain boundaries, which indicates a higher grain strength compared to intercrystalline interlayers. MA led to an increase in the average grain size to $\sim 5\,\mu$m (Figure 4), which may indicate a change in the nature of sintering from solid-phase to liquid-phase sintering. Its source may be low-melting Bi-containing compounds of eutectic origin [13], which promote mass transfer during recrystallization sintering and more uniform crystallite growth.

Figure 5 shows the temperature dependences of the real part of the complex dielectric constant of the ceramics under study. In all samples, at $T < 600$ K, an increase in permittivity is observed with increasing temperature, ending in a blurred frequency-dependent maximum (T_m) corresponding to the phase transition (PT) from the paraelectric phase to the ferroelectric one. As the frequency of the measuring field increases, the maximum shifts to the high-temperature region. PT occurs in the temperature range of (700–800) K in the BFBT sample, and in the range of (650–750) K in BFBTm.

When approximating the dependencies $T_m(f)$ over the entire frequency range, we used the Vogel-Fulcher ratio (1):

$$f = f_0 \exp \frac{E_a}{k(T_m - T_{VF})}, \qquad (1)$$

where f_0 is the frequency of attempts to overcome the potential barrier E_a, k is the Boltzmann constant, and T_{VF} is the Vogel-Fulcher temperature, interpreted as the temperature of „static freezing“ of electric dipoles or transition to the state of a dipole glass. The best result was achieved with parameters $f_0 \sim 9.16 \cdot 10^9$ Hz and $f_0 \sim 1.96 \cdot 10^{11}$ Hz, $E_a \approx 0.04$ eV and $E_a \approx 0.08$ eV, and Vogel-Fulcher temperatures $T_{VF} \approx 692$ K and $T_{VF} \approx 636$ K for BFBT and BFBTm, respectively. The results obtained indicate that the studied SS exhibit relaxation behavior,

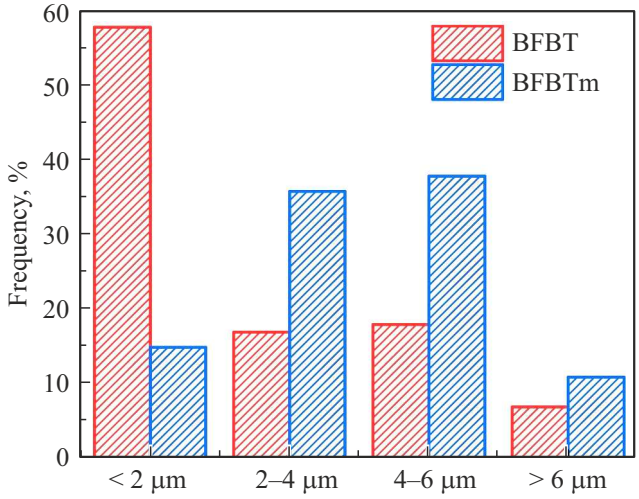

Figure 4. Grain size distribution in the ceramics under study.

which may be related to the presence of ion-rich regions in the ceramic crystal structure Bi^{+2} or Ba^{+2}.

We additionally analyzed the behavior of the dielectric constant using the Curie-Weiss law to describe the nature of the diffuse phase transition in the materials under study. Usually above the Curie temperature, the dielectric constant of a classical ferroelectric obeys the Curie-Weiss law and is defined as:

$$\varepsilon' = \frac{C}{(T - T_{CW})}, \quad (T > T_{CW}), \qquad (2)$$

where T_{CW} and C are the temperature and the Curie-Weiss constant, respectively. Figure 6 shows the behavior of the inverse value of the dielectric constant $(1/\varepsilon')$ as a function of temperature at a frequency of 100 kHz and the corresponding inserts illustrating the implementation of the Curie-Weiss law. The graph clearly shows that above the Burns temperature (T_B) all samples follow the linear Curie-Weiss law. The Burns temperature is the temperature

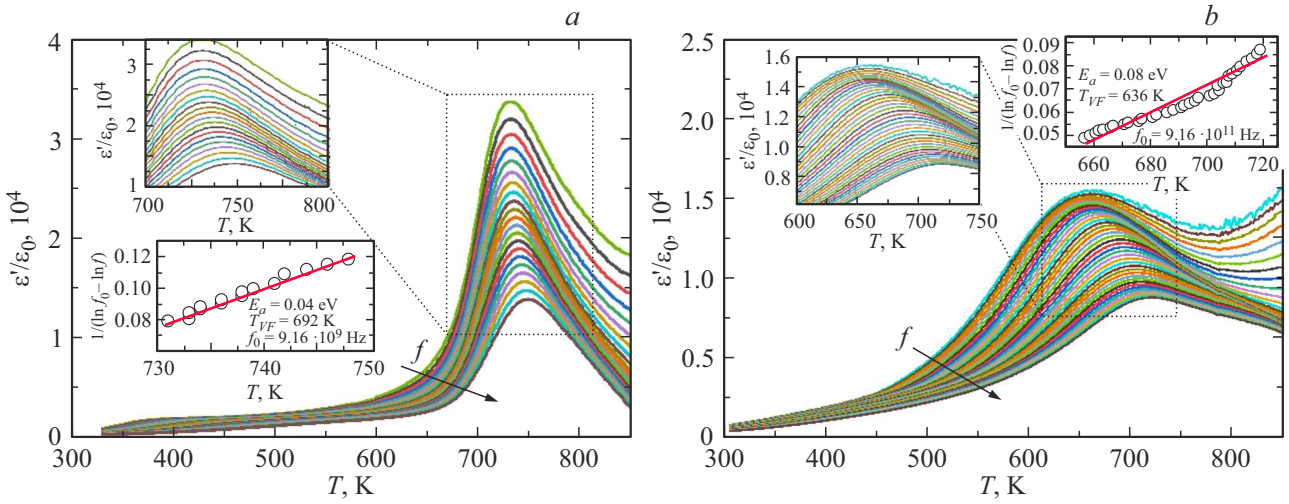

Figure 5. Temperature dependences of the real part of the complex dielectric constant for the compositions BFBT (left) and BFBTm (right). Inserts — fulfillment of the Vogel-Fulcher relation.

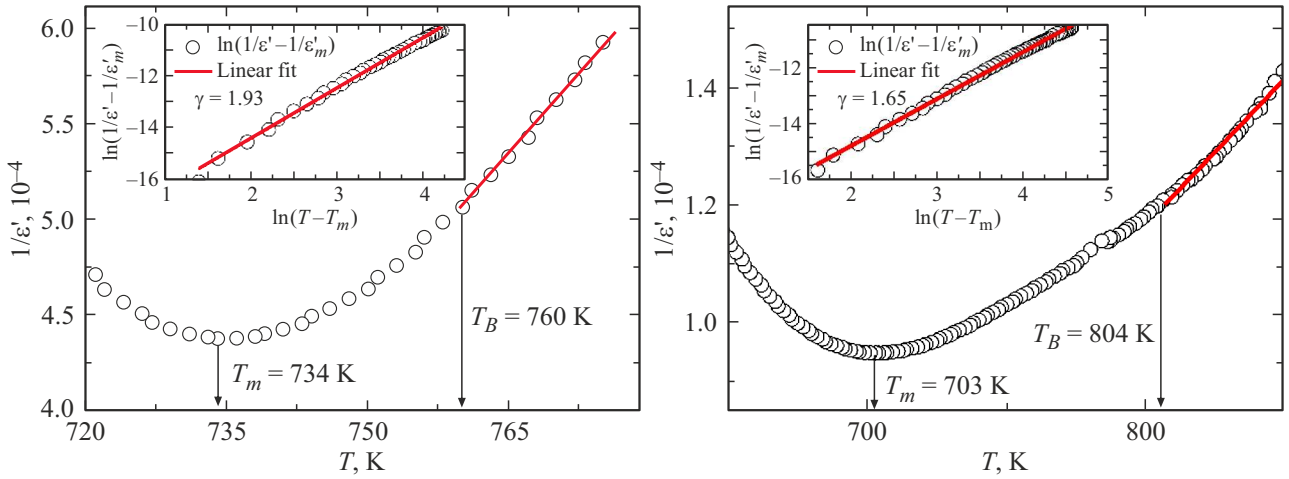

Figure 6. Temperature dependences of the inverse real part of the complex dielectric constant for ceramics BFBT (left) and BFBTm (right). Inserts — fulfillment of the Curie-Weiss law.

at which $1/\varepsilon'$ begins to deviate from the linear law. The obtained values of T_B after linear approximation are shown inside each graph in Figure 6 and indicate that mechanical activation shifts T_B into the low-temperature range. For a more accurate analysis of the relaxor behavior of ceramics, an approximation was performed using the modified Curie-Weiss law and the value of the critical index (γ) for PT from the FE phase to the PE phase was calculated. The modified Curie-Weiss law can be expressed as:

$$\frac{1}{\varepsilon'} - \frac{1}{\varepsilon'_m} = \frac{(T - T_m)^\gamma}{C}, \qquad (3)$$

where ε'_m, γ and C are the permittivity at T_m, the critical index and the Curie-Weiss constant, respectively. The value of γ ranges from 1 to 2, and if it is 1, then this is the case for an ideal relaxor ferroelectric, and the value of $\gamma \sim 2$ is typical either for a material with a disordered crystal structure or for an ideal redux ferroelectric. The insert of each graph in Figure 6 shows a graph of the dependence of $\ln(1/\varepsilon' - 1/\varepsilon'_m)$ on $\ln(T - T_m)$ and the calculated values of γ after linear approximation. The obtained values of γ are 1.93 and 1.65 for BFBT and BFBTm, respectively. For all samples, the values of γ are greater than 1.5, which indicates that the materials are of a relaxor nature. Thus, mechanical activation led to a more uniform dissolution of the SS components and the ordering of its structure.

The non-mechanically activated sample demonstrates extremely high conductivity, which is expressed in a sharp increase in the tangent of the dielectric loss angle after 400 K (Figure 7, *a*). In contrast to BFBT, the tangent of the dielectric loss angle in BFBTm is orders of magnitude lower. The cause of the observed effects may be oxidation of Fe ions and volatilization of Bi_2O_3, or Maxwell-Wagner relaxation resulting from the accumulation of free charges at the interface of regions rich in Bi or Ba.

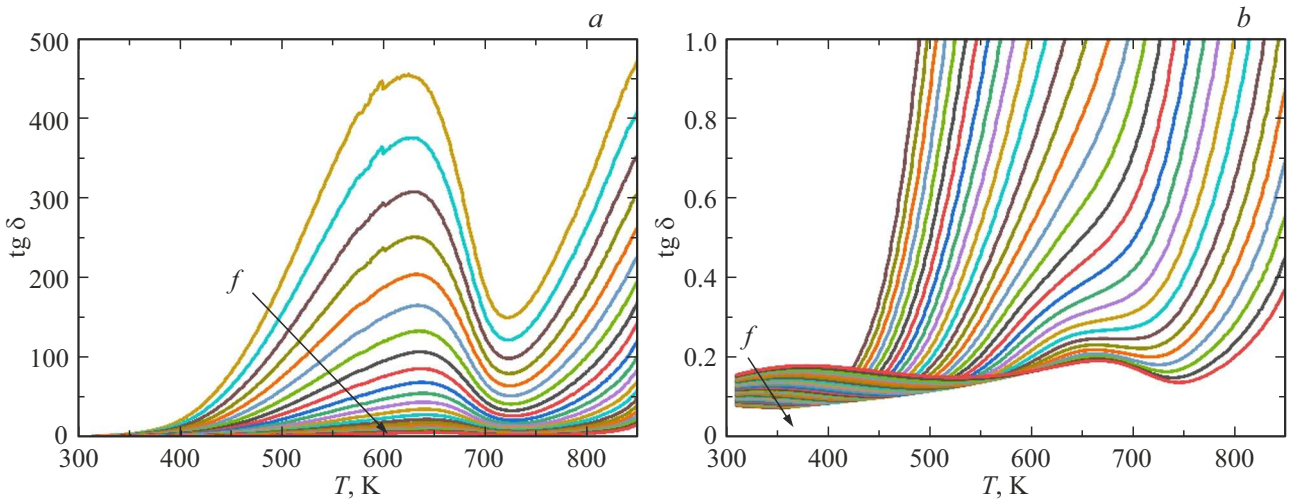

Figure 7. Temperature dependences of the tangent of the dielectric loss angle in BFBT (a) and BFBTm SS (b).

The PT blurring in the ceramics under study may be associated with increased crystallochemical disorder due to the presence of transition metal ions (Fe, Ti) in the structure of the ceramics under study. The resulting local fluctuations in the chemical composition by volume lead to the fact that the properties of the material change from one site to another, thereby causing PT blurring.

As part of the study, work was also carried out to create a polarized state in the studied samples using the „hot" polarization method. Due to the high conductivity, it was not possible to achieve a stable piezo response in the BFBT samples. The piezoelectric module value d_{33} in BFBTm ceramics was 120 pC/N, which is significantly higher than that of ceramics of the binary system $(1-x)$BF$-x$BT, manufactured using conventional ceramic technology [14].

4. Conclusion

Samples of ceramics from the binary system SS $(1-x)BiFeO_3-xBaTiO_3 + 2$ wt.% Bi_2O were obtained by solid-phase reactions followed by sintering using conventional ceramic technology using mechanical activation and without$_3$ ($x = 0.29$). X-ray studies have shown that the objects have a pseudocubic crystal structure at room temperature. Analysis of diffraction peaks showed the presence of diffuse scattering in non-mechanically activated samples, which indicates the presence of atomic segregation (the presence of regions in the crystal structure whose chemical composition differs from that of the main matrix). In the mechanically activated samples, the signs of segregation disappeared, and a more uniform distribution of $BaTiO_3$ was observed in the $BiFeO_3$ matrix, which led to the formation of two solid solutions with similar cell parameters. Mechanical activation also affected the grain structure, increasing the average grain size to $\sim 5\,\mu$m.

The study of dielectric characteristics revealed the behavior characteristic of ferroelectric relaxors. Blurred FE $\rightarrow$ PE phase transition occurred in the temperature range of (700–800) K in non-mechanically activated samples and (650–750) K in mechanically activated samples. Relaxation processes were approximated using the Vogel-Fulcher ratio with parameters $f_0 \sim 9.16 \cdot 10^9$ Hz and $f_0 \sim 1.96 \cdot 10^{11}$ Hz, $E_a \approx 0.04$ eV and $E_a \approx 0.08$ eV, and Vogel temperatures-Fulcher's $T_{VF} \approx 692$ K and $T_{VF} \approx 636$ K in samples produced with and without mechanical activation, respectively. We suggest that the relaxation-like behavior and blurring of the phase transition in the studied ceramics may be related to the presence of non-interacting regions with increased Bi or Ba content, differing in crystal lattice symmetry and chemical composition. The maximum values of the piezoelectric module were observed for mechanically activated ceramics ($\sim$ 120 pC/N). The results show that mechanically activated BF-BT ceramics with a superstoichiometric addition of bismuth may be a promising material for future applications.

Funding

The research was carried out with the financial support of the Russian Science Foundation (project No.24-22-00415) using the equipment of the Center for Collective Use of the Research Institute of Physics of the Southern Federal University.

Conflict of interest

The authors declare that they have no conflict of interest.

References

[1] A.P. Pyatakov, A.K. Zvezdin. UFN **182**, *6*, 593 (2012) (in Russian).
[2] J. Zhai, Z. Xing, S. Dong, J. Li, D. Viehland. Appl. Phys. Lett. **88**, 062510 (2006).

[3] S. Tehrani, J.M. Slaughter, M. Deherrera, B.N. Engel, N.D. Rizzo, J. John Salter, M. Durlam, R.W. Dave, J. Janesky, B. Butcher, K. Smith, G. Grynkewich. Proceedings of the IEEE **91**, *5*, 703 (2003).
[4] W.A. Borders, H. Akima, S. Fukami, S. Moriya, S. Kurihara, Y. Horio, S. Sato, H. Ohno. Applied Physics Express **10**, *1*, 013007 (2008).
[5] J. Chen, J. Cheng. J. Am. Ceram. Soc. **99**, 536 (2016).
[6] N.A. Boldyrev, E.I. Sitalo, L.A. Shilkina, A.V. Nazarenko, A.D. Ushakov, V.Y. Shur, L.A. Reznichenko, E.V. Glazunova. Ceramics, **6**, 1735 (2023).
[7] Y. Tian, F. Xue, Q. Fu, L. Zhou, C. Wang, H. Gou, M. Zhang. Ceram. Int. **44**, 4287 (2018).
[8] B. Yaffe, W. Cook, G. Yaffe. Piezoelektricheskaya keramika. M: Mir, 1974, p. 288 (in Russian).
[9] M. Ahart, M. Somayazulu, R.E. Cohen, P. Ganesh, P. Dera, H. Mao, R.J. Hemley, Y. Ren, P. Liermann, Z. Wu. Nature **451**, 545 (2008).
[10] M.M. Kumar, A. Srinivas, S.V. Suryanarayana. J. Appl. Phys. **87**, 855 (2000).
[11] K. Tong, C. Zhou, J. Wang, Q. Li, L. Yang, J. Xu, W. Zeng, G. Chen, C. Yuan, G. Rao. Ceram. Int. **43**, 3734 (2017).
[12] N.A. Boldyrev, E.S. Esin, L.A. Shilkina, S.I. Dudkina, A.V. Nagaenko, L.A. Reznichenko. Ceramics **8**, 7 (2025).
[13] N.A. Boldyrev, A.V. Pavlenko, L.A. Shilkina, A.V. Nazarenko, A.A. Bokov, L.A. Reznichenko, A.G. Rudskaya, E.I. Panchenko. Ceramics International **45**, *12*, 14768 (2019).
[14] N.A. Boldyrev, A.V. Pavlenko, L.A. Shilkina et al. Izvestiya Rossijskoj akademii nauk. Seriya fizicheskaya **80**, *11*, 1469 (2016) (in Russian).

Translated by A.Akhtyamov